Symmetric eikonal model for projectile-electron excitation and loss in relativistic ion-atom collisions

A.B.Voitkiv and B.Najjari

Max-Planck-Institut für Kernphysik,
Saupfercheckweg 1, D-69117 Heidelberg, Germany

V.P.Shevelko

P.N.Lebedev Physical Institute of the Russian Academy of Sciences,
Leninsky Avenue 53, 117924 Moscow, Russia

Abstract

At impact energies $\gtrsim 1$ GeV/u the projectile-electron excitation and loss occurring in collisions between highly charged ions and neutral atoms is already strongly influenced by the presence of atomic electrons. In order to treat these processes in collisions with heavy atoms we generalize the symmetric eikonal model, used earlier for considerations of electron transitions in ion-atom collisions within the scope of a three-body Coulomb problem. We show that at asymptotically high collision energies this model leads to an exact transition amplitude and is very well suited to describe the projectile-electron excitation and loss at energies above a few GeV/u. In particular, by considering a number of examples we demonstrate advantages of this model over the first Born approximation at impact energies $\sim$ 1–30 GeV/u, which are of special interest for atomic physics experiments at the future GSI facilities.

PACS numbers: 34.10+x, 34.50.Fa

I. INTRODUCTION

During the last two decades there has been performed a large number of experimental investigations of projectile-electron excitation and loss in collisions between relativistic highly charged ions and solid and gaseous targets. In particular, a variety of very heavy projectiles with the net charge 52 – 91 a.u. were used in the experiments. The experiments have also covered a very large interval of impact energies ranging from comparatively low relativistic energies of $\sim$ 100-200 MeV/u [1]-[4] to extreme relativistic energy of 160 GeV/u [6]-[8] where the projectile velocity already only fractionally differs from the speed of light $c = 137$ a.u..

Most of the data, however, have been collected for impact energies not exceeding a few hundreds of MeV/u. For impact energies above 1 GeV/u there exists just a few experimental results. They include the data on the electron loss from 10.8 GeV/u Au^{78+}(1s) ions penetrating solid targets [9]-[10] and on the electron loss from 160 GeV/u Pb^{81+}(1s) ions colliding with solid [6] and gaseous [7] targets.

Besides, one should also note that the experimental data on the elementary cross sections in collisions at very high energies collected using solid targets are not very accurate. The loss cross sections, reported for 160 GeV/u Pb^{81+}(1s) projectiles penetrating solid and gas targets differ between themselves roughly by a factor of 2 (see [6]-[7]). The reason for this difference, as was recently explained in [11], lies in multiple collisions suffered by the projectiles when they move in solids which does not allow one an accurate experimental determination of the values for elementary ion-atom cross sections. In the case of 10.8 GeV/u Au^{78+}(1s) ions the data of [9] and [10], which were both collected for collisions with solid state targets, also differ by about of a factor of 2 (but the reason for this is not completely clear).

Concerning difficulties in the theoretical description of the ion-atom collisions, there should be mentioned two main points, which complicate the treatment of the projectile-electron excitation and loss: The presence of atomic electrons and the fact that in case of collisions with a heavy atom the atomic field may be too strong making it necessary to go beyond the first Born approximation.

The latter point is known to be of extreme importance when considering the projectile-electron excitation and loss processes occurring in collisions of very highly charged ions with heavy atoms at relatively low impact energies 0.1 – 0.2 GeV/u, where the difference between experimental data and first Born calculations reaches an order of magnitude. At such energies, however, the atomic electrons play only a minor role in the projectile-electron transitions and their presence can simply be neglected [13].

With increase in the impact energy the role of the higher order effects in the projectile-target interaction diminishes. Nevertheless, even at energies well above 1 GeV/u the first Born approximation tends to substantially overestimate transition probabilities and the accuracy of first Born results for cross sections remains unclear, especially in the case when the collision causes more than one electron of the projectile to undergo transitions. Besides, at such impact energies even for the most highly charged projectiles (like e.g. hydrogen-like uranium ions) the influence of the electrons of the atom on the projectile-electron transitions can no longer be ignored [13].

In the present paper we shall demonstrate that the so called symmetric eikonal (SE) model, extended to account for the presence of atomic electrons, can be used for treating the projectile-electron excitation and loss in collisions with heavy atoms at impact energies $\gtrsim$ 1 GeV/u. In particular, we will show that in the limit of asymptotically high impact energies the transition amplitude, derived in the SE model, coincides with the amplitude obtained in

the light cone approximation which means that the SE model provides essentially an exact solution for the problem of projectile-electron excitation and loss in extreme relativistic ion-atom collisions.

The forthcoming upgrade of the heavy-ion facilities at GSI (Darmstadt, Germany) will allow one to perform extensive experimental explorations of the different aspects of heavy ion – atom collisions at impact energies in the range 1 – 30 GeV/u. It will be seen below that in this range of impact energies the SE model represents a very valuable tool for describing the projectile-electron excitation and loss in collisions with very heavy atoms.

Atomic units are used throughout unless otherwise stated.

II.   THEORY

Depending on whether or not the electrons of the atom are 'active' in the collision, one normally distinguishes two atomic modes (see e.g. [12], [13]) which can contribute to the projectile-electron transitions. In one of them, which is often called *screening*, the electrons of the atom act coherently with the atomic nucleus screening (partially or fully) the field of the latter. The other mode, in which the atomic electrons actively participate undergoing transitions, is termed *antiscreening*. In this mode the behavior of the projectile-electron is influenced mainly by the electrons of the atom while the nucleus of the atom plays only a minor role [14].

In collisions with heavy atoms, which are of special interest for the present article, the antiscreening mode is much weaker than the screening one and below will not be considered. In the screening mode the field of the atom can be regarded as external that enables one to reduce a many-electron problem of the ion-atom collision to a problem of the motion of the electron of the projectile in two external fields: the field of the nucleus of the ion and the field of the atom. The latter is taken as a superposition of the field of the atomic nucleus and the field of the atomic electrons whose space distribution is assumed to be 'frozen' during the very short collision time [13].

In the rest frame of the ion the electron is described by the Dirac equation

$$i\frac{\partial \Psi(\mathbf{r},t)}{\partial t} = \hat{H}\Psi(\mathbf{r},t). \tag{1}$$

The Hamiltonian $\hat{H}$ reads

$$\hat{H} = \hat{H}_0 + \hat{W}, \tag{2}$$

where

$$\hat{H}_0 = c\boldsymbol{\alpha}\cdot\mathbf{p} + \beta c^2 - \frac{Z_I}{r} \tag{3}$$

is the Hamiltonian for the electron motion in the field of the ionic nucleus and

$$\hat{W} = \boldsymbol{\alpha}\cdot\mathbf{A}(\mathbf{r},t) - \Phi(\mathbf{r},t) \tag{4}$$

is the interaction between the electron and the field of the atom. In the above expressions $\boldsymbol{\alpha}$ and β are the Dirac's matrices, $\mathbf{r}$ coordinates of the electron with respect to the ionic nucleus, Φ and $\mathbf{A}$ are, respectively, the scalar and vector potentials of the electromagnetic field of the incident atom.

The field of the atom in its rest frame is described by the scalar potential which, using results of [15] and [16], can be taken as

$$\Phi' = \frac{Z_A \phi(r')}{r'}, \tag{5}$$

where

$$\phi(r') = \sum_j A_j \exp(-\kappa_j r') \tag{6}$$

with the screening parameters A_j ($\sum_j A_j = 1$) and κ_j given in [15] and [16]. We assume that in the rest frame of the ion the atom moves along a classical straight-line trajectory $\mathbf{R} = \mathbf{b} + \mathbf{v}t$, where $\mathbf{b} = (b_x, b_y)$ is the impact parameter and $\mathbf{v} = (0, 0, v)$ the atomic velocity. Using Eqs.(5)-(6) and the Lorentz transformation for the potentials we obtain that in the rest frame of the ion the potentials of the atomic field are given by

$$\Phi(\mathbf{r}, t) = \frac{\gamma Z_A}{\sqrt{\gamma^2(z - vt)^2 + (\mathbf{r}_\perp - \mathbf{b})^2}} \sum_j A_j \exp\left(-\kappa_j \sqrt{\gamma^2(z - vt)^2 + (\mathbf{r}_\perp - \mathbf{b})^2}\right).$$

$$\mathbf{A}(\mathbf{r}, t) = \left(0, 0, \frac{v}{c}\Phi\right) \tag{7}$$

where γ is the collisional Lorentz factor and $\mathbf{r} = (\mathbf{r}_\perp, z)$ with $\mathbf{r}_\perp \cdot \mathbf{v} = 0$.

Within the SE model the transition amplitude is approximated by

$$a_{fi}(\mathbf{b}) = -i \int_{-\infty}^{+\infty} dt \langle \chi_f(t) \mid \left(\hat{H} - i\partial/\partial t\right) \chi_i(t) \rangle, \tag{8}$$

where the initial and final states of the electron, whose motion in the field of the ionic nucleus is affected by the field of the atom, are chosen according to

$$\chi_i(t) = \psi_0 \exp(-i\varepsilon_0 t) \exp\left(i \int_{-\infty}^{t} dt' \Phi(t')\right)$$

$$\chi_f(t) = \psi_n \exp(-i\varepsilon_n t) \exp\left(i \int_{+\infty}^{t} dt' \Phi(t')\right). \tag{9}$$

Here, ψ_0 and ψ_n are the initial and final undistorted states of the electron in the ion.

Making use of the fact that the dependence of the scalar potential Φ on the electron coordinates and time is of the form $\Phi = \gamma Z_A f(s_\perp, \gamma|z - vt|)$, where $\mathbf{s}_\perp = \mathbf{r}_\perp - \mathbf{b}$ the transition amplitude (8) can be transformed into

$$a_{fi}(\mathbf{b}) = i\frac{c}{v} \int_{-\infty}^{+\infty} dt \exp(i\omega_{n0} t) \left\langle \psi_n \left| \exp\left(i \int_{-\infty}^{+\infty} dt' \Phi(t')\right) \times \right.\right.$$

$$\left.\left. \left(\frac{\Phi(t)}{\gamma^2}\alpha_z - v\left(\nabla_\perp \int_{-\infty}^{t} dt' \Phi(t')\right) \cdot \boldsymbol{\alpha}_\perp\right) \right| \psi_0 \right\rangle, \tag{10}$$

where $\omega_{n0} = \varepsilon_n - \varepsilon_0$ is the electron transition frequency and $\nabla_\perp$ denotes the two-dimensional (in the (x, y)-plane) gradient operator.

The amplitude (10) can be simplified by employing the relation

$$\lim_{\lambda \to +0} \int_{-\infty}^{+\infty} dt \exp(i\omega_{n0} t) \exp(-\lambda|t|) \int_{-\infty}^{t} dt' \Phi(t')$$

$$= \frac{i}{\omega_{n0}} \int_{-\infty}^{+\infty} dt \exp(i\omega_{n0} t) \Phi(t), \quad (\omega_{n0} \neq 0), \tag{11}$$

4

that yields

$$a_{fi}(\mathbf{b}) = i\frac{c}{v} \int_{-\infty}^{+\infty} dt \exp(i\omega_{n0}t) \left\langle \psi_n \left| \exp\left(i \int_{-\infty}^{+\infty} dt' \Phi(t')\right) \times \right.$$
$$\left. \left(\frac{\Phi(t)}{\gamma^2} \alpha_z - i\frac{v}{\omega_{n0}} \left(\nabla_\perp \Phi(t)\right) \cdot \boldsymbol{\alpha}_\perp\right) \right| \psi_0 \right\rangle. \tag{12}$$

A. The Limit of weak interaction

If the interaction between the electron of the ion and the atom is sufficiently weak one can replace the exponent $\exp\left(i \int_{-\infty}^{+\infty} dt' \Phi(t')\right)$ in (12) by 1. Then integrating in (12) by parts over the space and using the continuity equation

$$\frac{\partial \rho_{n0}}{\partial t} + \nabla_\perp \cdot \mathbf{j}_{n0} = 0 \tag{13}$$

for the transition charge and current densities,

$$\rho_{n0} = \psi_n^\dagger \psi_0 \exp\left(i\omega_{n0}t\right)$$
$$\mathbf{j}_{n0} = \psi_n^\dagger c\boldsymbol{\alpha} \psi_0 \exp\left(i\omega_{n0}t\right), \tag{14}$$

we obtain

$$a_{fi}(\mathbf{b}) = i\frac{c}{v} \int_{-\infty}^{+\infty} dt \exp(i\omega_{n0}t) \left\langle \psi_n \left| \frac{v}{c}\Phi + \alpha_z \left(\frac{\Phi}{\gamma^2} - i\frac{v}{\omega_{n0}} \frac{\partial \Phi}{\partial z}\right) \right| \psi_0 \right\rangle. \tag{15}$$

Taking into account that $\frac{\partial \Phi}{\partial z} = -\frac{1}{v}\frac{\partial \Phi}{\partial t}$ and

$$\int_{-\infty}^{+\infty} dt \exp\left(i\omega_{n0}t\right) \frac{\partial \Phi}{\partial t} = -i\omega_{n0} \int_{-\infty}^{+\infty} dt \exp\left(i\omega_{n0}t\right) \Phi \tag{16}$$

we arrive at the transition amplitude

$$a_{fi}(\mathbf{b}) = i \int_{-\infty}^{+\infty} dt \exp(i\omega_{n0}t) \left\langle \psi_n \left| \Phi \left(1 - \frac{v}{c}\alpha_z\right) \right| \psi_0 \right\rangle \tag{17}$$

which coincides with expression for the amplitude obtained in the first Born approximation.

B. The High-Energy Limit

An important question, which will be addressed in this subsection, concerns the high-energy limit $(\gamma \to \infty)$ of the SE model. Keeping in mind that $\Phi = \gamma Z_A f(s_\perp, \gamma|z - vt|)$ one can show that

$$\int_{-\infty}^{+\infty} dt \exp(i\omega_{n0}t)\Phi(t) = \frac{2Z_A}{v} \exp\left(i\omega_{n0}z/v\right) \int_{-\infty}^{+\infty} d\xi f(s_\perp, \xi)$$
$$= \exp\left(i\omega_{n0}z/v\right) G\left(s_\perp, \frac{\omega_{n0}}{\gamma v}\right), \tag{18}$$

5

where at the moment the explicit form of the function G is not important. Correspondingly,

$$\int_{-\infty}^{+\infty} dt \ \Phi(t) = G(s_\perp, 0) \equiv G_0(s_\perp). \tag{19}$$

At sufficiently large impact energies, where the difference between $G = G\left(s_\perp, \frac{\omega_{n0}}{\gamma v}\right)$ and G_0 essentially vanishes, we can replace the amplitude (12) by the following expression

$$\begin{aligned} a_{fi}(\mathbf{b}) &= i\frac{c}{v\gamma^2} \langle \psi_n | \exp(iG) \exp(i\omega_{n0}z/v) \, G \, \alpha_z | \psi_0 \rangle \\ &- i\frac{c}{\omega_{n0}} \langle \psi_n | \exp(iG) \exp(i\omega_{n0}z/v) \, (\nabla_\perp G) \cdot \boldsymbol{\alpha}_\perp | \psi_0 \rangle. \end{aligned} \tag{20}$$

We now take the second line of (20), integrate there by parts, use the continuity equation (13) and then again integrate by parts. As a result of these manipulations, expression (20) transforms into

$$\begin{aligned} a_{fi}(\mathbf{b}) &= \left\langle \psi_n \left| \exp(i\omega_{n0}z/v) \exp(iG) \left(1 - \frac{v}{c}\alpha_z\right) \right| \psi_0 \right\rangle \\ &- \frac{c}{v\gamma^2} \langle \psi_n | \exp(i\omega_{n0}z/v) \exp(iG) (1 - iG) \alpha_z | \psi_0 \rangle. \end{aligned} \tag{21}$$

The limit $\gamma \to \infty$ of the amplitude (21) is given by

$$a_{fi}(\mathbf{b}) = \left\langle \psi_n \left| \exp(i\omega_{n0}z/v) \exp(iG_0) \left(1 - \frac{v}{c}\alpha_z\right) \right| \psi_0 \right\rangle \tag{22}$$

and it coincides with the transition amplitude derived in the so called light-cone approach (see [17], [13]).

The light-cone approach is strictly valid at $\gamma \to \infty$ and in this limit enables one to solve the problem of electron loss (ionization) and excitation exactly. One should also mention that the case of a strong ion-atom interaction this exact solution does not coincide with the first Born results, no matter how high is the impact energy [13]. Taking the above two points into account we can make the following conclusions. First, in the high-energy limit the SE model yields an exact solution for the transition amplitude of the projectile-electron excitation and loss. Second, even at $\gamma \to \infty$ the results of the SE model still in general differ from those of the first Born approximation.

It is rather obvious that such conclusions would also hold if the electron transitions in the ion are caused by the collision with a charged particle (e.g. a stripped atomic nucleus) and, for instance, can be applied to K-shell ionization of atoms by high-energy bare nuclei. In this respect one should note that in the literature on relativistic ion-atom collisions there had been already attempts to consider the high-energy limit of distorted-wave models for the case of atomic ionization or excitation by the impact of a nucleus, where these processes are treated as a three-body Coulomb problem (the incident and atomic nuclei and atomic electron). In particular, starting with the work of [18]-[20], it had been assumed that the high-energy limit of such distorted-wave models for ionization and excitation processes, like the continuum-distorted-wave-eikonal-initial-state (CDW-EIS) (see e.g. [21], [22]) and the SE, is simply that of the first Born approximation.

We have just seen, however, that for the SE model this is not true and that in the high-energy limit the transition amplitude, obtained in this model, goes over into the amplitude derived in the light-cone approach. Since at $\gamma \gg 1$ the CDW-EIS model becomes essentially identical to the SE, the high-energy limit of the CDW-EIS coincides with the light-cone approach but differs from the first Born approximation.

C. The explicit form of the amplitude

Using the explicit form (7) of the scalar potential we obtain that

$$\int_{-\infty}^{+\infty} dt \exp(i\omega_{n0}t)\Phi(t) = \frac{2Z_A}{v} \exp\left(i\omega_{n0}z/v\right) \sum_j A_j K_0\left(s_\perp \Lambda_j\right), \tag{23}$$

where where K_0 is the modified Bessel function [23], $s_\perp = |\mathbf{s}_\perp| = |\mathbf{r}_\perp - \mathbf{b}|$ and

$$\Lambda_j = \sqrt{\kappa_j^2 + \omega_{n0}^2/(\gamma^2 v^2)}. \tag{24}$$

Besides, it also follows from (23) that

$$\int_{-\infty}^{+\infty} dt \Phi(t) = \frac{2Z_A}{v} \sum_j A_j K_0\left(\kappa_j \, s_\perp\right). \tag{25}$$

Taking Eqs.(23) and (25) into account the transition amplitude becomes

$$
\begin{aligned}
a_{fi}(\mathbf{b}) &= i\frac{2Z_A c}{v^2} \sum_j A_j \left\langle \psi_n \left| \exp\left(i\frac{\omega_{n0}z}{v}\right) \exp\left(i\frac{2Z_A}{v} \sum_j A_j K_0\left(\kappa_j \, s_\perp\right)\right) \times \right. \right. \\
&\qquad \left. \left. \left(\frac{\alpha_z}{\gamma^2} K_0\left(s_\perp \Lambda_j\right) - i\frac{v\Lambda_j}{\omega_{n0}s_\perp} K_1\left(s_\perp \Lambda_j\right) \, \mathbf{s}_\perp \cdot \boldsymbol{\alpha}_\perp \right) \right| \psi_0 \right\rangle,
\end{aligned} \tag{26}
$$

where K_1 is the modified Bessel function [23].

D. The limit of vanishing screening

The results obtained above, can also be applied for treating ionization and excitation of neutral atoms in relativistic collisions with bare nuclei. This can be done by setting in (26) $\kappa_j = 0$, replacing there Z_A by Z_N, where Z_N is the charge of the nucleus incident on the atom, and regarding now ψ_0 and ψ_n as the initial and final states of the 'active' electron of the atom. Keeping in mind that $\sum_j A_j = 1$, taking into account that $K_0(x) \approx -\ln\left(\frac{x}{2}\right) - \Gamma$ for $| x | \ll 1$ (see e.g. [23]), where Γ is Euler's constant, and disregarding an inessential phase-factor we obtain

$$
\begin{aligned}
a_{fi}(\mathbf{b}) &= i\frac{2Z_N c}{v^2} \left\langle \psi_n \left| \exp\left(i\frac{\omega_{n0}z}{v}\right) \exp\left(-i\frac{2Z_A}{v} \ln s_\perp\right) \times \right. \right. \\
&\qquad \left. \left. \left(\frac{\alpha_z}{\gamma^2} K_0\left(\frac{\omega_{n0}}{\gamma v} s_\perp\right) - i\frac{v\Lambda_j}{\omega_{n0}s_\perp} K_1\left(s_\perp \Lambda_j\right) \, \mathbf{s}_\perp \cdot \boldsymbol{\alpha}_\perp \right) \right| \psi_0 \right\rangle.
\end{aligned} \tag{27}
$$

III. APPLICATIONS

The SE model is normally regarded as a tool for describing collision-induced transitions between bound states. In our case it would mean that this model should be first of all applied for treating the projectile-electron excitation. It is known [24] that at comparatively low relativistic impact energies the model has a problem with describing transitions
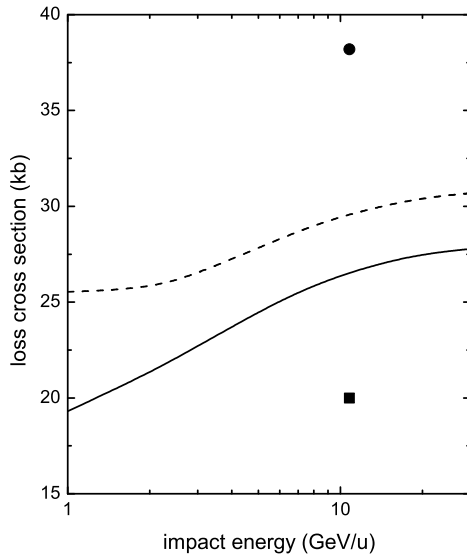
FIG. 1: Cross section for the electron loss from $Au^{78+}(1s)$ ions in collisions with neutral Au atoms. Solid curve: eikonal results. Dash curve: first Born results. The circle displays experimental data from [9] while the square shows the result of [10] scaled to the gold target.

involving electron spin flip. However, this problem diminishes when the energy increases and practically disappears at energies $\gtrsim 1$ GeV/u.

The SE model can also be used for considering the projectile-electron loss (in particular, the total cross section). In such a case the model also becomes more accurate when the impact energy increases. In particular, provided in the rest frame of the atom the magnitude of the velocity of the electron, emitted by the projectile, is of the order of the collision velocity, the SE model can be applied for calculating not only the total but also differential loss cross sections. In practical terms this condition holds starting already with $\gamma \simeq 2$–3, i.e. at impact energies ~ 1–2 GeV/u.

As was shown in the previous section, at asymptotically high impact energies the SE model yields an exact solution. In the case of the projectile-electron excitation and loss in collisions with neutral atoms even for the most highly charged projectiles the region of such energies is actually reached already at $\gamma \sim 30$–50. Thus, the model should work excellently starting with the magnitude of γ of a few tens.

Taking all this into account one can expect that the SE model performs quite well at impact energies ~ 1–30 GeV/u, which are of special interest for the present study. Below the projectile-electron excitation and loss will be considered in this energy range for collisions between hydrogen- and helium-like highly charged ions and heavy atoms by using the SE model. Results of this model will also be compared with those of the first Born approximation.

A.   Single-electron loss

In figure 1 we show results for the electron loss from incident $Au^{78+}(1s)$ projectiles in collisions with neutral Au atoms at impact energies 1-30 GeV/u. These results include our

first Born and eikonal calculations as well as experimental data from [9] and [10] on the electron loss from 10.8 GeV/u $Au^{78+}(1s)$ projectiles.

In the case considered our eikonal and first order results differ by 15-35%. As expected, when the impact energy increases the difference between them decreases. On overall, the difference is not large but nevertheless should be taken into account if precise cross section values are needed.

Both the first Born and eikonal cross sections agree neither with the experimental data of [9] nor with that of [10]. The data from [9] are substantially smaller (by about of 30%–50%) while the data reported in [10] are considerably larger (by about a factor of 1.3–1.4) than our results [25].

As was already mentioned in the Introduction, there is a difference by roughly a factor of 2 between experimental cross sections reported for for the loss from 160 GeV/u Pb^{81+} ions in collisions with solid and gas targets with the solid state cross sections being larger. The origin of this difference, which was explained in [11], lies in multiple collisions between the projectile and atoms inside solids which effectively enhance the electron loss process. Since the magnitude of this difference depends on the impact energy and decreases when the energy decreases, similar reasons are probably responsible for the observed disagreement between our results for atomic targets and the experimental data from [10].

B.   Two-electron transitions

If a projectile-ion initially carries several electrons, then more than one electron of the ion can be simultaneously excited and/or lost in a single collision with a neutral atom. Helium-like ions are simplest projectiles, for which simultaneous transitions of more than one electron are possible, and below we consider double electron loss and loss-excitation for the case of such projectiles.

It is known (see e.g. [13]) that, provided the condition $\frac{Z_I Z_A}{v} > 0.4$ is fulfilled, two-electron transitions in a heavy helium-like ion occurring in collisions with an atom are governed practically solely by the independent interactions between the atom and each of the electrons of the ion. In order to describe such transitions one can apply the independent electron model. According to this model the cross section for the double electron loss from a helium-like ion is given by

$$\sigma_{l,l} = 2\pi \int_0^\infty db\, b P_{l,l}(b), \tag{28}$$

where the probability $P_{l,l}(b)$ for the two-electron loss is given by

$$P_{l,l}(b) = P_{loss}^2(b), \tag{29}$$

where $P_{loss}(b)$ is the single-electron loss probability in a collision with a given value of the impact parameter b.

The cross section for the simultaneous loss-excitation in the case of a helium-like ion is evaluated as

$$\sigma_{e,l} = 2\pi \int_0^\infty db\, b P_{e,l}(b), \tag{30}$$

where the probability $P(b)$ for the two-electron process is given by

$$P_{e,l}(b) = 2\, P_{exc}(b)\, P_{loss}(b), \tag{31}$$

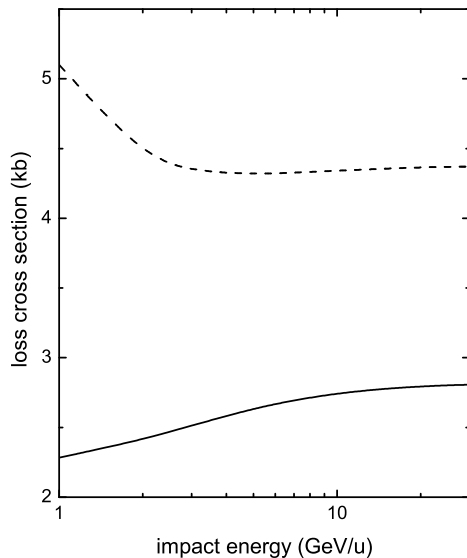where $P_{exc}(b)$ is the single-electron excitation probability.

9

FIG. 2: Cross sections for double electron loss from $Au^{77+}(1s^2)$ ions in collisions with neutral Au atoms. Solid curve: eikonal results. Dash curve: first Born results.

1. Double-electron loss

Figure 2 shows calculated cross sections for double electron loss from $Au^{77+}(1s^2)$ projectiles incident on neutral Au atoms at impact energies 1–30 GeV/u. Compared to the single loss, now the difference between the eikonal and first Born results is much more pronounced. For impact energies $\sim 1 - 5$ GeV/u these calculations predict even qualitatively different dependencies of the cross sections on the collisions energy. The absolute difference between the first Born and eikonal cross sections ranges between $\simeq 2.5$ at 1 GeV/u to $\simeq 1.5$ at 30 GeV/u. Moreover, as additional calculations show, for impact energies above 30 GeV/u the ratio of $\simeq 1.5$ remains almost a constant and, thus, even at asymptotically high collision energies the first Born calculation still substantially overestimates the cross section values.

2. Simultaneous loss-excitation

In figure 3 we present results of calculations for the simultaneous projectile-electron excitation and loss, $U^{90+}(1s^2) \rightarrow U^{91+}(n = 2, j) + e^-$, where n and j are, respectively, the principal quantum number and the total angular momentum of the excited state of the hydrogen-like ion. The projectile is assumed to collide with Kr, Xe and Au atomic targets at an impact energy of 20 GeV/u. Similarly to the case of the double electron loss, considered above, we observe that the differences between the cross sections, calculated with the first Born and eikonal probabilities, can be quite substantial if the atom is sufficiently heavy. For collisions leading to the population of the states with $j = 1/2$ the first Born results are larger by a factor of $\simeq 1.16$ (Kr), $\simeq 1.38$ (Xe) and $\simeq 1.84$ (Au). When the states with $j = 3/2$ are populated this ratio is $\simeq 1.12$, $\simeq 1.31$ and $\simeq 1.67$, respectively.

We see that the difference between the first Born and eikonal cross sections turns out to be somewhat smaller for transitions involving the states with $j = 3/2$. This can be attributed
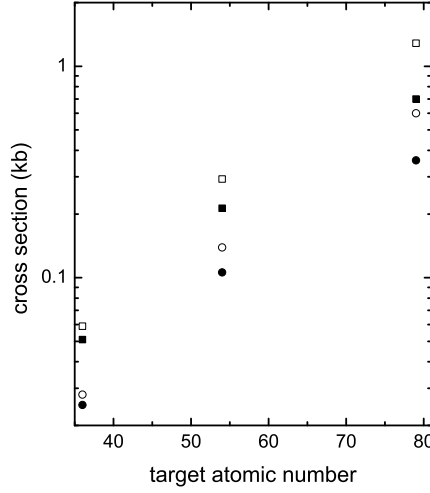
10

FIG. 3: Cross sections for the simultaneous electron loss-excitation, $U^{90+}(1s^2) \to U^{91+}(n = 2, j)$ + e^-, occurring in collisions with Kr, Xe and Au atomic targets at 20 GeV/u. $j = 1/2$ and $j = 3/2$ are the angular momentum of the states of the hydrogen-like uranium ion. Squares and circles show results for $j = 1/2$ and $j = 3/2$, respectively. Open and solid symbols denote the cross sections obtained using the first Born approximation and the SE model, respectively.
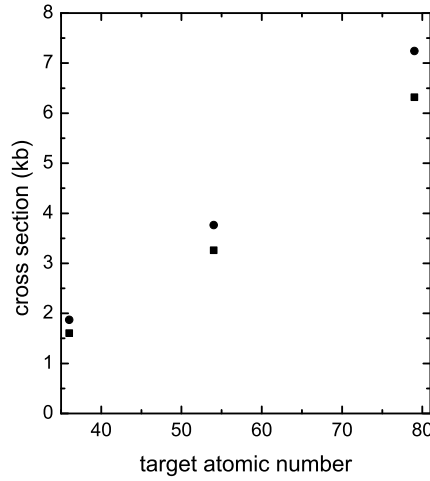

FIG. 4: Cross sections for excitation of 20 GeV/u $U^{91+}(1s)$ projectiles into the states with $n = 2, j = 1/2$ (squares) and $n = 2, j = 3/2$ (circles) in collisions with Kr, Xe and Au atomic targets. The cross sections were calculated using the SE model.

to the fact that, compared to the $j = 1/2$ case, these transitions are characterized by larger impact parameters. As a result, the field of the atom acting on the electrons of the ion is weaker and, therefore, the first Born treatment becomes less inaccurate.

As additional calculations show, the differences between the results of the eikonal and first Born calculation does not substantially change when the impact energy increases further. Thus, like for the double electron loss, even at asymptotically high impact energies the first Born calculation may considerably overestimate the cross section for the simultaneous
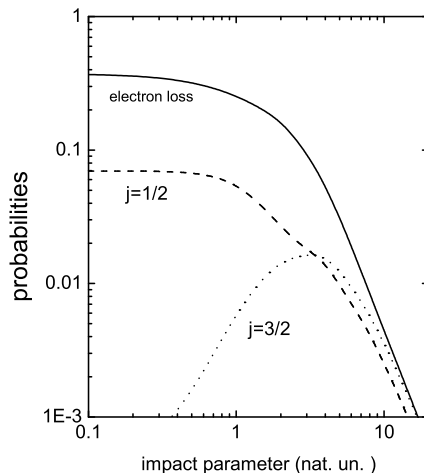
11

FIG. 5: Probabilities for the electron loss, excitation to the states with ($n = 2$, $j = 1/2$) and ($n = 2$, $j = 3/2$) in collisions of 20 GeV/u U^{91+}(1s) ions with Au atoms.

projectile-electron excitation and loss.

According to both the first Born and eikonal results the cross sections for the simultaneous loss-excitation are larger for transitions to the states with $j = 1/2$. However, the pure excitation U^{90+}(1s) $\rightarrow$ U^{90+}(1s; n=2, j) (or the excitation U^{91+}(1s) $\rightarrow$ U^{91+}(n=2, j), see figure 4) at these rather high energies proceeds already more efficiently into the states with $j = 3/2$. The origin of this interesting peculiarity can be understood by considering the single-electron transition probabilities. It turns out that the probability for the electron loss has a larger overlap with the probability for the excitation into the states with $j = 1/2$ (see for illustration figure 5).

IV. CONCLUSIONS

We have considered the symmetric eikonal model for treating projectile-electron transitions in relativistic collisions with heavy atoms.

We have shown that at asymptotically high impact energies this model yields the same results as the light-cone approach and, thus, offers an exact solution for the transition amplitude. In the limit $\gamma \gg 1$ another popular distorted-wave model – the continuum-distorted-wave-eikonal-initial-state approximation – becomes essentially identical to the symmetric eikonal model. Therefore, at asymptotically high impact energies the CDW-EIS also becomes exact and, contrary to what was stated earlier, does not coincide with the first Born approximation.

Using the SE model and the first Born approximation we have calculated cross sections for the projectile-electron excitation and loss. We have shown that at impact energies $\sim$ 1–30 GeV/u, which are relevant for the future GSI facility, there are noticeable deviations between the eikonal and first Born results for single-electron transitions and very substantial differences between such results for transitions involving two projectile electrons. Moreover, these very substantial differences 'survive' even in the asymptotic limit $\gamma \rightarrow \infty$.

Our results clearly show a great advantage of the SE model over the first Born approximation.

12

Acknowledgment

---

[1] R. Anholt, W.E. Meyerhof, X.-Y. Xu, H. Gould, B. Feinberg, R.J. McDonald, H.E. Wegner and P. Thieberger, Phys. Rev. **A 36** 1586 (1987); W.E. Meyerhof, R. Anholt, X.-Y. Xu, H. Gould, B. Feinberg, R.J. McDonald, H.E. Wegner and P. Thieberger, NIM **A 262** 10 (1987)

[2] Th. Stöhlker et al, Nucl. Instr.Meth. **B 124** 160 (1997)

[3] C. Scheidenberger and H. Geissel, Nucl. Instr.Meth. **B 135** 25 (1998)

[4] C. Scheidenberger, Th. Stölker, W.E.Meyerhof, H. Geissel, P.H. Mokler and B. Blank, Nucl. Instr.Meth. **B 142** 441 (1998)

[5] T. Ludziejewsky, T.Stöhlker, C.D.Ionesku, P.Rymuza, H.Beyer, F.Bosch, C.Kozhuharov, A.Krämer, D.Liesen, P.H.Mokler, Z.Stachura, P.Swiat, A.Warczak, R.W.Dunford, Phys. Rev. **A 61** 052706 (2000)

[6] H.F. Krause, C.R. Vane, S. Datz, P. Grafström, H. Knudsen, S. Scheidenberger, and R.H. Schuch, Phys. Rev. Lett. **80**, 1190 (1998)

[7] H.F. Krause, C.R. Vane, S. Datz, P. Grafström, H. Knudsen, U. Mikkelsen, S. Scheidenberger, R.H. Schuch, and Z. Vilakazi, Phys. Rev. **A 63** 032711 (2001)

[8] C.R.Vane and H.F.Krause, NIM **B 261** 244 (2007)

[9] A. Westphal and Y.D.He, Phys.Rev.Lett. **A 71** 1160 (1993)

[10] N. Claytor, A. Belkacem, T. Dinneen, B. Feinberg, and H. Gould, Phys.Rev. **A 55** R842 (1997)

[11] A.B. Voitkiv, B. Najjari, and A. Surzhykov, J.Phys. **B 41** 111001 (2008)

[12] E.C. Montenegro, W.E. Meyerhof and J.H. McGuire, Adv.At.Mol. and Opt. Phys. **34** 249 (1994)

[13] A. B. Voitkiv and J. Ullrich, *Relativistic Collisions of Structured Atomic Particles* (Springer-Verlag, Berlin, 2008)

[14] According to first Born considerations, in the antiscreening mode the nucleus of the atom does not at all interact with the electron of the projectile.

[15] G. Moliere, Naturforsch. **2A** 133 (1947)

[16] F. Salvat, J.D. Martinez, R. Mayol, and J. Parellada, Phys.Rev.**A 36** 467 (1987)

[17] A.J.Baltz, Phys.Rev.Lett. **78**, 1231 (1997).

[18] G.R.Deco and N.Grün, J.Phys. **B 22** 1357 (1989)

[19] G.R.Deco, K.Momberger and N.Grün, J.Phys. **B 23** 1990 (1989)

[20] G.R.Deco and N.Grün, J.Phys. **B 22** 3709 (1989)

[21] D.S.F. Crothers, *Relativistic Heavy-Particle Collision Theory*, Kluwer Academic/Plenum Publishers, London (2000)

[22] A.B.Voitkiv and B.Najjari, J.Phys. **B 40** 3295 (2007)

[23] M. Abramowitz and I. Stegun, *Handbook of Mathematical Functions* (Dover Publications, Inc., New York, 1965)

[24] A.B.Voitkiv, B.Najjari and J.Ullrich, Phys.Rev. **A 75** 062716 (2007)

[25] Note that the experimental data reported in [10] are in a very good agreement with results of theoretical considerations of [26] and [27]. However, the theoretical models of [26] and [27],

which were developed for collisions between individual ions and atoms (and, therefore, should be first of all tested in collisions with gas targets), overestimate experimental data obtained in collisions with rarefied gas targets [7] by a factor of 2-3 (while our results agree very nicely with this atomic target experiment). The critical discussion of the models of [26] and [27] can be found in [13].

[26] R. Anholt and U. Becker, Phys.Rev. **A 36** 4628 (1987)
[27] A.H. Sørensen, Phys.Rev. **A 58** 2895 (1998)